2023 IEEE 47th Annual Computers, Software, and Applications Conference (COMPSAC) | 979-8-3503-2697-0/23/$31.00 ©2023 IEEE | DOI: 10.1109/COMPSAC57700.2023.00074

Positioning Vectors for Mobile Ad-Hoc Positioning

Yerkezhan Sartayeva
Department of Computing
The Hong Kong Polytechnic University
Hong Kong, China
yerkezhan.sartayeva@connect.polyu.hk

Yunfei Liu
Department of Computing
The Hong Kong Polytechnic University
Hong Kong, China
yunfei.liu@connect.polyu.hk

Yik Him Ho
Department of Computing
The Hong Kong Polytechnic University
Hong Kong, China
yh.ho@connect.polyu.hk

Henry C. B. Chan
Department of Computing
The Hong Kong Polytechnic University
Hong Kong, China
cshchan@comp.polyu.edu.hk

***Abstract*—In recent years, there has been considerable interest in indoor positioning with the advent of smartphones. Conventional indoor positioning methods are mostly infrastructure-based and non-collaborative. With the recent development of Ultra-WideBand (UWB) technologies, highly accurate distance and orientation detection have become available for supporting collaborative positioning, a new positioning paradigm. Hence there is a strong need to study collaborative positioning, which is referred to in this paper as mobile ad-hoc positioning (MAP). To contribute to the development of MAP, we present novel positioning vectors with the potential to tackle many related collaborative positioning problems and open an interesting area of research. Our contributions are outlined as follows. First, we present the concept of positioning vectors with the foundational features. Second, we present both experimental and simulation results, illustrating the use of positioning vectors. In particular, we discuss a COVID-19 related case study on social distancing. Last but not least, we discuss the future research directions of positioning vectors. In summary, this paper provides valuable insights into the development of MAP in general and positioning vectors in particular.**

Keywords—indoor positioning, collaborative positioning, mobile ad-hoc positioning, positioning vectors

I. Introduction

With the popularity of mobile location-based services, there has been considerable interest in indoor positioning. Conventional indoor positioning methods are in general infrastructure-oriented and non-collaborative, but as portable devices such as smartphones are becoming more computationally powerful, collaborative positioning has attracted researchers' attention because of its merits, such as reduced dependence on infrastructure, a higher localization rate because more nodes can be reached, etc. Non-collaborative positioning methods can be broadly classified as proximity-based [1], geometric-based ([2], [3]) and fingerprint-based [4] and typically use fixed coordinates, while relative coordinates can be used in collaborative positioning systems, which create new and interesting positioning problems. In this paper, we propose a novel positioning paradigm for collaborative positioning, where, given mobile terminals that can estimate the distance and orientation of other mobile terminals, the relative positions of mobile terminals are determined using positioning vectors. To the best of our knowledge, this positioning paradigm has not been thoroughly studied before. Our work is inspired by the fact that, in recent years, the latest iPhone models [5] and high-end models of Android phones [6] can both provide UWB capability, allowing the detection of other UWB-based mobile terminals in terms of orientation and distance. In fact, compared to Bluetooth Low Energy (BLE), accuracy can be significantly improved i.e., from meter-level to centimeter-level accuracy ([7], [8]). It is expected that UWB can become as popular as BLE in the near future, providing a more powerful positioning service, particularly through collaborative positioning. Hence, there is a strong need to study collaborative positioning methods, in particular, a basic framework for its research and development. This paper seeks to contribute to this goal by presenting or introducing positioning vectors. Our contributions are summarized as follows. First, we introduce positioning vectors for mobile ad-hoc positioning (MAP). To the best of our knowledge, this paper is among the first that extensively studies the use of vectors for collaborative positioning or mobile ad-hoc positioning purposes. Second, we present experimental and simulation results to illustrate the positioning vector methods. In particular, we` present COVID-19 related use cases to illustrate an application of positioning vectors. The organization of the remaining sections of this paper is outlined as follows. Section II presents the related work on collaborative positioning methods. Section III introduces the positioning vector theory. Sections IV and V present experimental results and simulation results, respectively. Section VI outlines future research work/directions. Finally, Section VII presents the conclusion.

II. Related Work

There is a wide variety of collaborative solutions proposed in the literature. For example, [9] developed a message passing algorithm for collaborative localisation of wireless sensor nodes, where ranging was performed with the help of the signal's Time of Arrival (ToA). [10] designed a graph neural network, which takes the adjacency matrix of network nodes as input, meaning it takes the layout of the network into account, where each edge between two nodes represents the distance between them. However, [10] did not take the angle of signal propagation into account in its adjacency matrix. When it comes to studies that are more similar to our work, one example is WAIPO [11], a collaborative IPS for smartphones. The system fuses WiFi fingerprints with magnetic fingerprints and uses the social information of people in the vicinity as well as images of their surroundings to localize people carrying smartphones, achieving a 87.3% accuracy rate. LocSpeck [12] also relies on a UWB ad-hoc network with WiFi fingerprinting but uses UWB transceivers instead of smartphones. Another cluster of similar works focuses on the localisation of mobile agents, e.g., in mobile ad-hoc networks (MANETs) and vehicular ad-hoc

979-8-3503-2697-0/23/$31.00 ©2023 IEEE
DOI 10.1109/COMPSAC57700.2023.00074

Authorized licensed use limited to: University of Waterloo. Downloaded on September 18,2023 at 07:05:25 UTC from IEEE Xplore. Restrictions apply.

networks (VANETs) ([13], [14], [15], [16]). For example, [13] designed a general multi-hop task offloading method for MANETs to distribute computational tasks among nodes. While there have been other works on using vectors for positioning purposes (e.g., [14] also used the idea of vector addition for tackling a positioning case for UWB-equipped unmanned aerial vehicles), we seek to provide a more comprehensive and fundamental study of positioning vectors in general and to consider relative or collaborative positioning using smartphones. In summary, inspired by the related work, this paper studies a vector-inspired approach to complement the previous research work with a focus on collaborative positioning.

III. Positioning Vectors

In this section, we present the novel concept of positioning vectors for mobile ad-hoc positioning (MAP). It is expected that positioning vectors can be applied to solve various collaborative positioning problems for MAP and provide the basic framework for future research. We assume there are *N* mobile terminals (i.e., M_1, M_2, … M_N) in the MAP system. Each mobile terminal can measure the distance and orientation to another mobile terminal within its coverage area subject to some errors (e.g., based on UWB). To measure orientation, it is assumed that the mobile terminals can determine the west-east direction (i.e., x-axis) such as when using a compass. Through these measurements, positioning vectors can be determined as discussed below.

A. Actual, Measured and Generated Positioning Vectors

We define $M_xM_y^{(a)}$ as the actual positioning vector for mobile terminals M_x and M_y. For example, the positioning vector $M_1M_2^{(a)}$ for mobile terminals M_1 and M_2 is as shown in Fig. 1. In vector form, we have:

$$M_1M_2^{(a)} = \left(r_{12}^{(a)}\cos(\theta_{12}^{(a)})\right)i + \left(r_{12}^{(a)}\sin(\theta_{12}^{(a)})\right)j \quad (1)$$

where $r_{12}^{(a)}$ and $\theta_{12}^{(a)}$ denote the ground truth distance and orientation from M_1 to M_2, respectively ($r_{xy}^{(a)} = \left\|M_xM_y\right\|_2$). θ_{12} is measured with respect to the x-axis (i.e., west-east direction). Due to the addition property of vectors, we have the following relationship:

$$M_xM_y^{(a)} = M_xM_k^{(a)} + M_kM_y^{(a)} \quad (2)$$

For instance, in Fig. 1, we have $M_1M_3^{(a)} = M_1M_2^{(a)} + M_2M_3^{(a)}$, which is represented by the perfect triangle. In practice, relative to itself, each mobile terminal can only determine the positions of other mobile terminals based on the measured positioning vectors. For example, the measured positioning vector for mobile terminals M_1 and M_2 is defined as $M_1M_2^{(m)}$, as shown in Fig. 1. Due to measurement errors, the measured positioning vectors usually deviate from the actual positioning vectors. If the user of M_1estimates the position of M_2 based on the measured positioning vector, the positioning error (e.g., in terms of root mean squared error) can be computed based on the difference between the actual and estimated positioning vectors. When combined, measured vectors between every pair of mobile terminals form a vector graph.

Based on the measured positioning vectors, we define an intermediate generated positioning vector as follows:

$$M_xM_y^{(g_{x,k,y})} = M_xM_k^{(m)} + M_kM_y^{(m)} \quad (3)$$

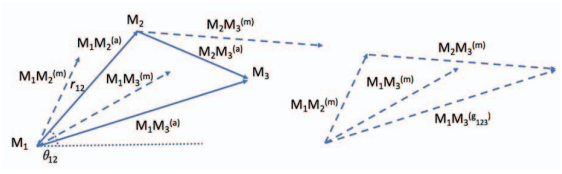

Fig. 1. Actual, measured and generated positioning vectors.

For example, Fig. 1 (right figure) shows one intermediate generated positioning vector for M_1 and M_3 based on the measured positioning vectors $M_1M_2^{(m)}$and $M_2M_3^{(m)}$. Note that, depending on the number of mobile terminals in the system and hence the number of combinations, there can be multiple intermediate generated positioning vectors. In general, we can determine the overall generated positioning vector as follows:

$$M_xM_y^{(g)} = \frac{1}{C_{xy}+1}\left(M_xM_y^{(m)} + \sum_k M_xM_k^{(m)} + M_kM_y^{(m)}\right) \quad (4)$$

That means, this generated positioning vector can be used to determine the position of M_y with respect to M_x taking into consideration the directly measured positioning vectors and all other measured positioning vectors (i.e., the overall mean), not just $M_xM_y^{(m)}$, where C_{xy} is the number of possible combinations for the other measured positioning vectors. In equation (3), we consider adding two vectors, which is referred to as degree 2 addition. In general, degree *n* addition can be performed by adding *n* vectors. If a generated vector cannot be determined based on degree 2 addition, the minimum degree *n* addition should be found, which can be done by means of Dijkstra's algorithm. In some cases, a node may not be connected to any other nodes. In this case, for example, if $M_xM_y^{(m)}$ is available, $M_yM_x^{(g)}$ can be estimated as $-M_xM_y^{(m)}$. In the worst case, a node may be totally disconnected from a vector graph, in which case its relative position cannot be estimated at all.

B. Orientation Vector and Coverage Area

An important consideration in positioning vector theory is that a mobile terminal, e.g., a UWB-equipped iPhone, can only detect other mobile terminals within its coverage area, so some measured vectors might be unavailable. As stated by Apple [17], UWB on iPhones has only a limited direction field of view, which allows the phones to measure the relative angle of other phones within around ±50° from the back. A relative angle < 0 indicates that the other terminal is on the left, and a relative angle > 0 indicates that the other terminal is on the right. We define an orientation vector for modeling this important property. For a mobile terminal M_x, its orientation vector is denoted as ϕ_x, which defines its detection direction as well as the coverage area. The magnitude of ϕ_x denotes the longest distance at which M_x can detect another terminal M_y. For example, as shown in Fig. 2, the orientation vector ϕ_1 points γ_1 degrees north-east and has a half-angle of β_1, thus defining the coverage area of M_1, the boundaries of which are denoted with

Authorized licensed use limited to: University of Waterloo. Downloaded on September 18,2023 at 07:05:25 UTC from IEEE Xplore. Restrictions apply.

dotted blue lines. Similarly, ϕ_2 can be defined for M_2 with its coverage denoted with dotted green lines. As the two coverage areas overlap, M_1 and M_2 can detect each other. Specifically, we can determine the angle between an orientation vector and an actual positioning vector such as ϕ_1 and $M_1M_2^{(a)}$, which is θ'_{12} in this case (all notations in the figure are related to the actual vector $M_1M_2^{(a)}$). We refer to θ'_{12} as the relative angle between M_1 and M_2. As $\theta_{12}{}'$ is less than β_1, M_1 can detect M_2. Similarly, θ'_{21} is less than β_2, so M_2 can detect M_1, but if M_2 did not face M_1, it would not be able to detect M_1, so visibility is directional. Note that $\theta'_{12} \neq \theta_{12}$ since θ_{12} is the absolute angle with respect to the true west-east axis that defines M_1M_2, and it is calculated using the compass angle at M_1 (γ_1) and $\theta_{12}{}'$ as $\theta_{12} = 90 - \theta'_{12} - \gamma_1$. Also note that, based on Fig. 2, the compass angle at M_2 is $\gamma_2 = 180^0 + \gamma_1$ since they are tilted along the same axis with their backs facing each other. We assume that $\forall k : \gamma_k^{(m)} = \gamma_k^{(a)}$, i.e., compass measurements at mobile terminals have no error. Generating missing vectors based on equation (4) can increase nodes' visibility to one another.

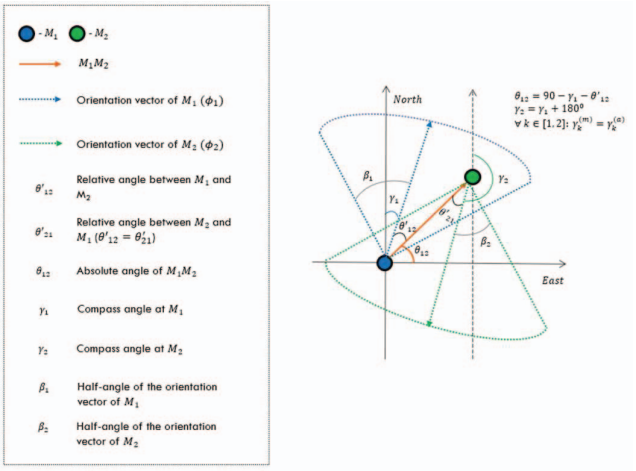

Fig. 2. Example of positioning vectors, orientation vectors and coverage areas.

IV. Experimental Results

To evaluate the proposed positioning vectors for MAP, we have conducted experiments in a computer laboratory. The size of the room is about 7 m × 12 m. The experiments were conducted with two UWB-equipped iPhones 11, which can measure distance and the relative angles between each other.

Positioning error is contingent on the accuracy of measured relative angle and distance between two phones, so these parameters were evaluated on the iPhones. Fig. 2 illustrates the experimental setup and shows that the two phones were placed such that they were tilted along the same axis with respect to the north-south axis and with their backs facing each other. Let M_1 and M_2 denote the two phones. Measurements were collected in the same environment in the same conditions in three iterations to obtain the average error. Four types of obstacles were placed between the two phones, namely: (1) a fabric chair (with a back of 3 cm in thickness), (2) a wooden door (5 cm in thickness), (3) a glass wall (under 1 cm in thickness) as well as (4) a 40-page stack of A4 papers. These obstacles were selected because they did not preclude UWB ranging during data collection, meaning that, despite the obstacles, both distance and relative angle measurements were available, whereas with a concrete wall or a whiteboard, for example, this would not be the case. In addition, two cases were considered: (C1) the ground truth relative angle between the two phones was fixed at 0° and the distance was set to values in the range [2 m, 6 m, 12 m, 18 m, 24 m, 30 m]; (C2) the ground truth distance between the two phones was fixed at 1 m and the relative angle was set to values in the range [±10°, ±20°, ±30°, ±40°, ±50°]. Note that, due to the test environment constraints and larger distance values, data on the influence of wood and glass on distance estimation in C1 could not be collected. Let $r_{xy} = \|M_xM_y\|_2$ be the distance and θ'_{xy} be the relative angle between phones M_x and M_y, respectively ($x \neq y$). Also note that $r_{xy}^{(a)} = r_{yx}^{(a)}$, but this does not necessarily hold for measured distances. Distance error ϵ_r and relative angle error $\epsilon_{\theta'}$ were thus calculated as follows:

$$\epsilon_r = \sqrt{\frac{\left(r_{12}^{(a)} - r_{12}^{(m)}\right)^2 + \left(r_{21}^{(a)} - r_{21}^{(m)}\right)^2}{2}} \quad (5)$$

$$\epsilon_{\theta'} = \sqrt{\frac{\left(\theta'_{12}{}^{(a)} - \theta'_{12}{}^{(m)}\right)^2 + \left(\theta'_{21}{}^{(a)} - \theta'_{21}{}^{(m)}\right)^2}{2}} \quad (6)$$

Results for distance error and relative angle error are shown in Fig. 3 and Fig. 4, respectively. For consistency across different settings, comparison was done against different relative angles rather than absolute angles (in different settings, even though the relative angles were configured to be the same, the phones did not always face the same direction with respect to the east). In all figures in this section, "distance" on the x-axis refers to the ground truth distance between the two phones, i.e., $|M_1M_2|^{(a)} = |M_2M_1|^{(a)}$, while "angle" on the axis refers to the ground truth relative angle between the two phones.

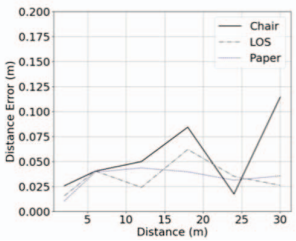

Fig. 3. Distance error between 2 phones for different distances (case C1).

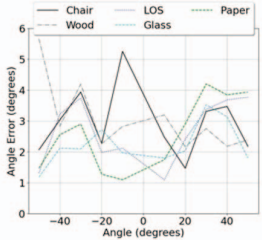

Fig. 4. Relative angle error between 2 phones for different relative angles (case C2).

Fig. 3 suggests that the largest deviation of a single distance estimate from the ground truth was under 12 cm, even for distances as large as 30 m. Similarly, Fig. 4 shows that the highest relative angle error was under 6 degrees. However, an angle error of even 4 degrees, for example, could be significant for larger distances, and the combined effect of angle and distance error can be seen by converting distances and angles into vectors. Please refer to equation (1) and Fig. 2 to see how relative angle and distance can be converted into a vector.

Authorized licensed use limited to: University of Waterloo. Downloaded on September 18,2023 at 07:05:25 UTC from IEEE Xplore. Restrictions apply.

Based on the above discussion, the next phase of the experiment aimed to evaluate the combined effect of relative angle error and distance error on positioning performance in terms of vector error ϵ_v, which was calculated as follows:

$$\epsilon_v = \frac{1}{2}\left(\left\|M_1M_2^{(m)} - M_1M_2^{(a)}\right\|_2 + \left\|M_2M_1^{(m)} - M_2M_1^{(a)}\right\|_2\right) \quad (7)$$

To investigate vector error in different settings, the same cases, C1 and C2, were used. Fig. 5 and Fig. 6 show vector errors for C1 and C2, respectively, for the four different obstacles and line-of-sight conditions (LOS).

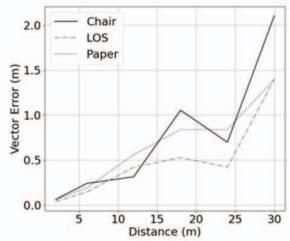

Fig. 5. Vector error vs distance with relative angle fixed at 0° (case C1).

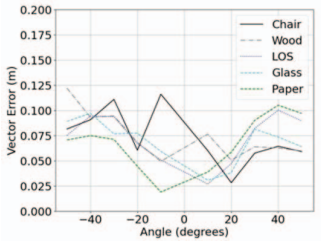

Fig. 6. Vector error vs relative angle with distance fixed at 1 m (case C2).

Fig. 5 demonstrates that, even though the relative angle error and distance error were small for a ground truth distance of 30 m, the vector error rose to over 2 m when there was a chair in the way. Even in LOS conditions, error for the same distance was under 1.5 m. Both paper and chair seemed to increase vector error, with the latter having a more significant effect, which makes sense because the chair was wider than the stack of papers. This can be explained by the relative angle error caused by the obstacles, which significantly increased the vector error, even though the relative angle error was low. However, for 12 m, the error was at most slightly over 50 cm for all settings, meaning that vector error becomes worse for larger distances, because errors in the relative angle become more expensive. Fig. 6 depicts the impact of the relative angle between two phones on vector error. The graph suggests that vector error tends to grow as the absolute value of the relative angle goes up, hence the "inverted triangle" shape, but overall, differences in error are not significant. In terms of obstacles, vector error was generally higher for wood and chair, with errors for the other two obstacles close to the LOS error.

V. SIMULATION RESULTS

In this section, we present simulation results on positioning vectors. The following shows representative results in two parts. In the first part, the aim is to study positioning errors for measured positioning vectors and generated positioning vectors under different situations. In the second part, a COVID-19-related use case on social distancing is presented to illustrate the application of positioning vectors. In general, unless otherwise specified, the simulation model is outlined as follows. We consider a coverage area of 10×10 m^2. In each simulation, N mobile terminals are randomly distributed over the coverage area. Hence, the actual positioning vectors can be determined. Based on the actual positioning vectors, the measured positioning vectors are determined based on some distance and angle errors. The distance and angle errors are based on a normal distribution model with a certain noise level relative to the true angle and magnitude values ($\Delta\theta$ and Δr for direction angle and vector magnitude, respectively). For example, for a vector $\vec{v} = 2i + 2j$, whose magnitude is $2\sqrt{2}$ and whose direction angle is 45°, if $\Delta\theta$ = 10%, then a normal distribution with a mean of zero and a standard deviation of $0.1 \times 45° = 4.5°$ will be formed, and a value from that distribution will be added to the original angle. The same applies to noise injection into vector magnitudes. For each mobile terminal, the orientation vector is determined by assuming that the vector points to the centroid of the remaining terminals. Root mean square error is used as the accuracy metric.

A. General Simulation Results

Fig. 7 compares the positioning errors for different percentages of distance error (graph on the left) and angle error (graph on the right) with a half-angle $\beta = 40^0$. In the first case, $\Delta\theta$ was set to 10%, and in the second case, Δr was set to 10% based on the normal distribution error model and the experimental results. The graph on the left demonstrates that, as expected, the positioning error for the measured positioning vectors is independent of the number of mobile terminals. By using the generated positioning vectors, significant improvement can be achieved, especially if Δr is high. For example, when there are 50 mobile terminals and Δr is 20%, the positioning error can be improved from around 1.4 m to 0.7 m (i.e., close to 100% improvement). This demonstrates the benefit of using collaborative positioning. If Δr is 5%, a positioning error of about 0.3 m can be achieved by using the generated positioning vectors. It is well known that the current BLE-based method can achieve a positioning error in the order of 1 m [18]. Therefore, this represents a significant improvement in positioning error. Similar to distance error, the right-hand graph in Fig. 7 shows the positioning error for different percentages of angle error. It is found that the results are similar. Fig. 8 shows the detection percentage for different angle errors and distance errors when the half angle is 40 degrees. It can be seen that for the measured positioning vectors, about 60% can be detected, which is not sensitive to the number of mobile terminals. For the generated positioning vectors, nearly 100% of the mobile terminals can be detected (i.e., using two positioning vectors). Furthermore, it is found that distance error and angle error have little effect on the minimum number of vectors required, but the number of mobile terminals has a slight effect. Fig. 9 further studies the minimum number of positioning vectors required for detection (i.e., the minimum number of hops to reach from one node to another node in the vector graph). As expected, the figure shows that the detection percentage depends on the half angle. With a half angle of 40°, about 60% of the mobile terminals can be detected directly (with just one positioning vector), while the majority of the other 40% require two hops. This shows that by using the generated positioning vector method, the relative position of all mobile terminals can be determined in most cases. This also

Authorized licensed use limited to: University of Waterloo. Downloaded on September 18,2023 at 07:05:25 UTC from IEEE Xplore. Restrictions apply.

indicates that the method should be scalable in terms of communication cost and computational cost as we only require a reasonable percentage of vectors to achieve a high detection rate. Further work will be conducted to study the scalability of the method.

Our results are consistent with similar works. For example, [14] also used vectors to localize nodes out of range and achieved an average localization error of 0.2 m in line-of-sight conditions with three UWB-equipped UAVs. The authors of [16] implemented relative positioning for three UWB-equipped robots and achieved a similar error of 0.4 – 0.5 m, but the robots were fully connected and used odometers. [15] fused UWB range and odometry measurements for relative localization of three robots, and their method yielded an accuracy rate of 0.15 m. It is difficult to compare these works to ours because they use different devices and UWB chips, and the number of terminals is different, but overall, the range of error is similar.

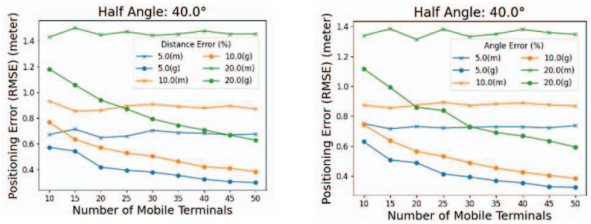

Fig. 7. Positioning error for different percentages of distance error (left figure) and angle error (right figure).

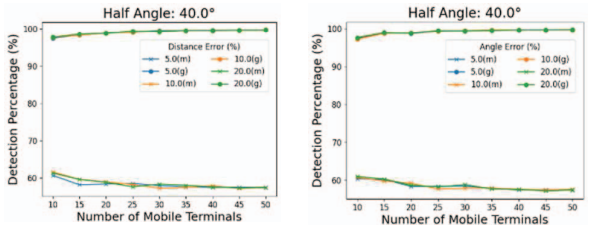

Fig. 8. Detection rate for different percentages of distance error (left figure) and angle error (right figure).

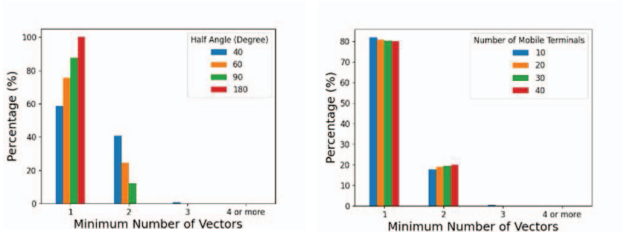

Fig. 9. Minimum number of positioning vectors required for detection for different half-angles (left figure) and number of terminals (right figure).

B. *COVID-19 Use Case – Social Distancing*

In this section, as an example, we present simulation results on a social distancing use case (i.e., related to COVID-19), which may also be extended to other similar use cases. Basically, a mobile user is considered safe (positive) if all other mobile terminals/users are more than 2 m away, meaning the actual positioning vectors to all other mobile terminals are over 2 m long. Based on the measured/generated positioning vectors, for each mobile terminal, there are four cases to be considered: (1) true positive (TP) - actual positioning vectors and measured/generated positioning vectors to all other mobile terminals are more than 2 m long; (2) true negative (TN) - at least one actual positioning vector and one measured/generated positioning vector to all other mobile terminals are within 2 m; (3) false positive (FP) - at least one actual positioning vector to another mobile terminal is within 2 m long but all measured/generated positioning vectors are more than 2 m long; (4) false negative (FN) - actual positioning vectors to all other mobile terminals are more than 2 m long but at least one measured/generated positioning vector to another mobile terminal is within 2 m long.

The following presents representative simulation results. In summary, Fig. 10 shows that when there are 10 or 20 mobile terminals over the coverage area, by means of measured positioning vectors, the false detection percentage is around 20% with mostly false positive cases. By means of generated positioning vectors, the false detection percentage can be reduced significantly, to less than 10%. In particular, the serious false positive percentage is reduced to a negligible percentage. When the number of mobile terminals increases, the true negative percentage increases, approaching 100%, meaning when the number of mobile terminals reaches a certain threshold, all mobile users will become unsafe. The above results show the advantages of using generated positioning vectors.

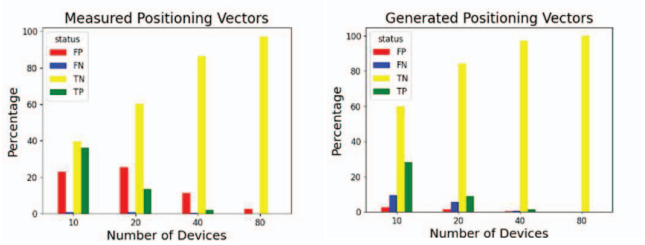

Fig. 10. Social distancing case study (TP, TN, FP, FN).

VI. Future Research Directions

In this section, we outline the future research directions of positioning vectors. First, while we present a generated approach for collaborative positioning, more advanced optimization algorithms should be explored, e.g., genetic algorithms, and they should be evaluated on actual UWB-equipped smartphones. For example, it is of interest to investigate using an image-inspired mechanism to transform a noisy vector graph to the close-to-actual vector graph. Secondly, it is important to conduct further research on vector graphs (e.g., fundamental properties). For example, there is a need to study an efficient algorithm to find all of the vectors for degree n addition between two nodes. Thirdly, in this paper, static positioning vectors are studied. As an extension, positioning vectors can be changed with respect to time (i.e., dynamic positioning vectors) because of the movement of the mobile terminals. By using dynamic positioning vectors, future positions of the mobile terminals, as well as their movements, can be tracked and predicted. This raises new and challenging research issues in this dynamic environment. Last but not least,

Authorized licensed use limited to: University of Waterloo. Downloaded on September 18,2023 at 07:05:25 UTC from IEEE Xplore. Restrictions apply.

the use of AI in general and machine learning in particular for positioning vectors should provide many interesting and challenging research problems e.g., using graph neural networks.

VII. Conclusion

In conclusion, this paper has presented a novel positioning vector framework for collaborative indoor positioning. One of the major advantages of the proposed approach is that relative position of mobile terminals can be determined collaboratively based on a vector-inspired approach, providing a new positioning paradigm (i.e., MAP). Real-life experiments have been conducted using UWB-equipped smartphones to demonstrate the feasibility and concept of using positioning vectors even with obstacles. Extensive simulations have been conducted to study the positioning error of positioning vectors in different situations, revealing their effectiveness. In particular, a COVID-19-related use case on social distancing was studied to demonstrate the application of positioning vectors. Last but not least, positioning vectors can provide many interesting and challenging research problems/issues for the research community.

Acknowledgments

This work has been supported by the Hong Kong PhD Fellowship Scheme provided by the Research Grants Council (RGC) of Hong Kong.

References

[1] F. Gu, X. Hu, M. Ramezani, D. Acharya, K. Khoshelham, S. Valaee and J. Shang, "Indoor localization improved by spatial context - a survey," *ACM Computing Surveys,* vol. 52, no. 3, 7 2019.

[2] N.-S. Duong and T.-M. D. Thi, "Smartphone indoor positioning based on enhanced BLE beacon multi-lateration," *TELKOMNIKA,* vol. 19, no. 1, pp. 51-62, 2021.

[3] Y. Hou, X. Yang and Q. H. Abbasi, "Efficient AoA-based wireless indoor localization for hospital outpatients using mobile devices," *Sensors,* vol. 18, no. 11, 2018.

[4] F. Zafari, A. Gkelias and K. K. Leung, "A survey of indoor localization systems and technologies," *IEEE Communications Surveys Tutorials,* vol. 21, no. 3, pp. 2568-2599, 2019.

[5] "Apple invents iBeacon version 2 using ultra-wide band radio technology," 2019. [Online]. Available: https://www.patentlyapple.com/patently-apple/2019/01/apple-invents-ibeacon-version-2-using-ultra-wide-band-radio-technology.html.

[6] M. Stone, "How does ultra-wideband work?," 25 August 2021. [Online]. Available: https://insights.samsung.com/2021/08/25/what-is-ultra-wideband-and-how-does-it-work-3/.

[7] F. Mazhar, M. G. Khan and B. Sällberg, "Precise indoor positioning using UWB: A review of methods, algorithms and implementations," *Wireless Personal Communications,* vol. 97, no. 3, pp. 4467-4491, 12 2017.

[8] J. Kolakowski, V. Djaja-Josko, M. Kolakowski and K. Broczek, "UWB/BLE tracking system for elderly people monitoring," *Sensors,* vol. 20, no. 6, 2020.

[9] S. Wang, F. Luo, X. Jing and L. Zhang, "Low-complexity message-passing cooperative localization in wireless sensor networks," *IEEE Communications Letters,* vol. 21, no. 9, pp. 2081-2084, 2017.

[10] W. Yan, D. Jin, Z. Lin and F. Yin, "Graph neural network for large-scale network localization," in *ICASSP 2021 - 2021 IEEE International Conference on Acoustics, Speech and Signal Processing (ICASSP)*, 2021.

[11] F. Gu, J. Niu and L. Duan, "WAIPO: A fusion-based collaborative indoor localization system on smartphones," *IEEE/ACM Transactions on Networking,* vol. 25, no. 4, pp. 2267-2280, 2017.

[12] M. Sakr, A. Masiero and N. El-Sheimy, "LocSpeck: A collaborative and distributed positioning system for asymmetric nodes based on UWB ad-hoc network and Wi-Fi fingerprinting," *Sensors,* vol. 20, no. 1, 2020.

[13] G. Feng, X. Li, Z. Gao, C. Wang, H. Lv and Q. Zhao, "Multi-path and multi-hop task offloading in mobile ad-hoc networks," *IEEE Transactions on Vehicular Technology,* vol. 20, no. 6, pp. 5347-5361, 2021.

[14] K. Guo, X. Li and L. Xie, "Ultra-wideband and odometry-based cooperative relative localization with application to multi-UAV formation control," *IEEE Transactions on Cybernetics,* vol. 50, no. 6, pp. 2590-2603, 2020.

[15] S. Zheng, Z. Li, Y. Liu, H. Zhang, P. Zheng, X. Liang, Y. Li, X. Bu and X. Zou, "UWB-VIO fusion for accurate and robust relative localization of round robotic teams," *IEEE Robotics and Automation Letters,* vol. 7, no. 4, pp. 11950-11957, 2022.

[16] M. Shalaby, C. C. Cossette, J. R. Forbes and J. Le Ny, "Relative position estimation in multi-agent systems using attitude-coupled range measurements," *IEEE Robotics and Automation Letters,* vol. 6, no. 3, pp. 4955-4961, 2021.

[17] Apple, "Initiating and maintaining a session," [Online]. Available: https://developer.apple.com/documentation/nearbyinteraction/initiating_and_maintaining_a_session.

[18] R. F. Brena, J. P. García-Vázquez, C. E. Galván-Tejada, D. Muñoz-Rodriguez, C. Vargas-Rosales and J. Fangmeyer, "Evolution of indoor positioning technologies: A survey," *Journal of Sensors,* vol. 2017, pp. 2630413:1-2630413:21, 2017.

Authorized licensed use limited to: University of Waterloo. Downloaded on September 18,2023 at 07:05:25 UTC from IEEE Xplore. Restrictions apply.